Simulations of some simple localised defects in alkali-doped alkaline-earth fluorides

1989 J. Phys.: Condens. Matter 1 10281

(http://iopscience.iop.org/0953-8984/1/51/005)

J. Phys.: Condens. Matter 1 (1989) 10281–10297. Printed in the UK

Simulations of some simple localised defects in alkali-doped alkaline-earth fluorides

A Amara, G Cremer, F Martin-Brunètiere and M Thuau
Laboratoire de Spectroscopie Atomique, URA 19, ISMRa, Université de Caen, 14032 Caen Cédex, France

Received 30 May 1989

Abstract. Using a simulation code for defective ionic crystals, the geometrical structure and the formation energies of some simple defects are calculated for alkali- (Li-, Na-, K-, Rb-) doped alkaline-earth fluorides (CaF_2, SrF_2); their migration, clustering and reorientation tendencies are also estimated. The alkali-interstitial–alkali-substitutional pair and the fluorine-vacancy–alkali-substitutional pair are the most probable defects. The ion-size effects of the alkali ions are discussed. We highlight the chief weakness of these defect models: our poor knowledge of the short-range interactions in these 'mixed' materials (alkali fluoride, alkaline-earth fluorides).

1. Introduction

Alkali-doped alkaline-earth fluoride crystals exhibit complicated optical spectra in the visible range after either additive or irradiation coloration and the behaviour of the spectrum is very confused under optical and (or) thermal treatment; thus the nature of the associated defects is somewhat disputed [1] and their configurations at the atomic scale are by no means certain. However, a very striking experimental fact is that the familiar colour centres (for instance F_2) of pure CaF_2 or SrF_2 cannot be observed in samples doped with a few 10^{-4} alkaline impurities and that they are replaced by entirely new centres which depend on the particular impurity. This fact strongly suggests that in doped fluorides the anion vacancies, which are the building blocks of colour centres, are concentrated in the immediate vicinity of the impurity ions. The impurity-ion–anion-vacancy cluster could pre-exist in the uncoloured doped crystals and capture electron(s) during the coloration process. Alternatively, the F centre (an anion vacancy with an electron) could be very mobile and strongly attracted by the alkaline impurities. So in a first approach the understanding of the defects in the coloured doped materials should probably be improved by the identification of the defects that are present in the doped crystals before the coloration process. To our knowledge the microscopic geometrical structure of the defects cannot be directly observed by experimental measurements. Moreover the experimental data analyses almost generally require the prior assumption of a microscopic defect model: consequently the microscopic description of the defects is confirmed by self-consistency arguments only. Thus the nature of the defects at the lattice scale cannot be worked out unequivocally from experimental data alone; Cormack [2] has highlighted these very complicated and ambiguous links between experimental observations, theoretical models of the defects, and microscopic knowledge of their configurations. Nevertheless there have been many attempts to determine

0953-8984/89/5110281 + 17 $02.50

the defect configurations in 'MF_2:A' crystals experimentally (alkaline-earth cation, M = Ca^{2+} or Sr^{2+}; alkali dopant, A = Li^+, Na^+, K^+ or Rb^+), mostly by measurements of conductivity, ionic thermocurrents, dielectric relaxation and nuclear magnetic resonance ([2–7] and references therein).

In the present work, by using a theoretical simulation, briefly summarised in § 2, we intend to forecast qualitatively (in § 3.1) which elementary defects are the most probable in uncoloured doped 'MF_2:A' crystals and what their migration ability is; § 3.2 describes their expected clusterings and the reorientation ability of some clusters and § 3.3 is devoted to studies of some possible mechanisms of 'AF' solution into 'MF_2' crystals. Throughout these studies we keep in mind the influence of both the nature of the alkali dopant and the host crystal. These defect simulations are based only on the experimental properties of the perfect crystals ('MF_2' and 'AF') through non-Coulombic ion interactions.

There have already been some similar studies, but they dealt with either only one impurity (mostly Na), only one host crystal (mostly 'CaF_2') or only a few types of defects. First Franklin [8] studied 'CaF_2:Na' with a rather crude model; then Catlow *et al* [9] made extensive computations on the undoped 'MF_2' system; Jacobs *et al* [10] dealt with 'CaF_2:A' using a method rather like ours; Bendall *et al* [11] performed almost the same study as ours but for the '$SrCl_2$:Na' system; finally Harding [12] improved the calculations for some defects in 'CaF_2:Na' by using a more rigorous approach.

2. Method

The energy added to the crystal by the defect formation, and the corresponding geometrical configuration, are calculated from the well known region strategy [3], set up in the HADES2 program [13]. The polarisable distortable static crystal is divided into concentric regions (I, IIA and IIB) around the localised defect. The self-energy of the outer regions (IIA+IIB) is harmonic with their ion displacements and the IIB self-energy is calculated in a continuum approximation using Mott and Littleton's theory [3, 14]. The ions of the inner regions (I+IIA) are described by the well known shell model (SM) [3, 15]. Their positions (core and shell) and their detailed mutual interactions (I–I, I–IIA) are explicitly calculated, using 'appropriate' non-Coulombic short-range interaction (SRI) potentials (shell–shell interaction between different ions and core–shell harmonic interaction on the same ion). The positions of the IIA charges are determined according to Mott and Littleton's approximation: the dielectric embedded charges are in equilibrium with the electric displacements created by all the charges forming the defect, whereas the implicit IIB region 'sees' only the net total charge of the defect. The ions (including the defect ones) in region I are iteratively relaxed using a fast Newton–Raphson procedure until they reach their zero-force positions.

The SM and SRI parameters for M and F ions in alkaline-earth fluorides are taken from Catlow *et al* [9]; like these authors, we neglect the 'M–M' SRI potential. Following Franklin [8], Bendall [11] and Harding [12], the SM parameters of the alkali dopant (A) and the SRI between A and F ions (and between A and A, should the occasion arise) are taken to be the same as those of the corresponding alkali fluoride (data set No 2 of Catlow *et al* [16]). Like the previous authors, we neglect the 'A–M' SRI, which is consistent with neglecting the 'M–M' SRI [9].

The cut-off of the SRI potentials is fixed at 1.51 lattice units (LU); the lattice unit is the nearest-neighbour (NN) fluorine distance in the 'MF_2' crystal [17]. The size of the

Table 1. Formation energies U(eV) of free intrinsic defects in MF_2 crystals.

MF_2		Anion Frenkel pair	Schottky trio	Cation Frenkel pair
CaF_2	This work	2.764	5.798	8.430
	[9]	2.75	5.75	8.00
	[12]†	2.81		
	[12]	2.71		
SrF_2	This work	2.368	5.912	7.911
	[9]	2.38	5.92	7.57
$SrCl_2$	[11]	2.05	3.98	5.85

† g_p (see text) extrapolated to 0 K.

I+IIA explicit region is about 2100 ions and the I region contains about 190 ions. Throughout the computations we take care to keep the region sizes constant and to centre them on the centre of the defect charges in order to avoid spurious energy contributions, particularly while comparing energies. The errors in the defect formation energies are a few tens of meV; but our errors are probably much lower when calculating a difference between energies that are computed by similar enough methods (e.g. height of the potential barrier between adjacent configurations). The accuracy of the ion positions is about 0.003 LU.

3. Results

We choose the following notation: V(X), I(X) and S(X) stand respectively for an X ion vacancy, an X ion in an interstitial site (an empty fluorine cube of the 'MF_2' crystal) and an X ion near the site of a missing ion of 'MF_2' (generally an M ion); X may be either F, a fluorine anion (F^-), A, an alkali-dopant cation (A^+), or M, the alkaline-earth cation (M^{2+}). The defects are termed 'free' if they are far enough from one another inside the host crystal that they do not interact and may be regarded as isolated in the crystal, and then their formation energies are simply additive. The defect formation energy U (always in eV) is the energy added to the crystal while creating the defect from the perfect crystal. We must remark that strictly speaking our computed energies U are the internal formation energies U_v at constant volume near the temperature 0 K, whereas the experimental formation energies are g_p, Gibbs' free enthalpy of formation at constant pressure and at somewhat higher temperatures. Harding [12] has already emphasised this important point.

3.1. Free elementary defects

We consider first the free intrinsic defects in undoped 'MF_2' crystals, then the free extrinsic defects in 'MF_2:A', and finally some migration energies.

3.1.1. Intrinsic defects. Table 1 compares with previous authors' calculations [9, 12] our results concerning the formation energies of the anion, [V(F)+I(F)], and cation, [V(M)+I(M)], Frenkel pairs and of the free Schottky trio [2V(F)+V(M)]. We note a satisfactory agreement between the results. The displacements of the surrounding ions do not exceed 0.10 LU. Except perhaps at very high temperature, the anion Frenkel pair is the only intrinsic localised disorder in 'MF_2' crystals, as has been commonly accepted for a long time [18].

Table 2. The simplest free extrinsic defects in 'MF_2: A' crystals.

(*a*) Substitutional: S(A)

MF_2	A	U (eV)	'On'- or 'off'-site, δ (LU) along ⟨100⟩	Barrier at [000]	Height (eV) along ⟨110⟩
CaF_2	Li^+	13.850	0.084	<0.001	≈0
	Na^+	14.421	on	—	—
	K^+	15.947	on	—	—
	Rb^+	17.255	on	—	—
SrF_2	Li^+	12.972	0.265	0.104	0.038
	Na^+	13.451	on	—	—
	K^+	14.495	on	—	—
	Rb^+	15.476	on	—	—
$SrCl_2$	Na^+	11.26 [11]			
	K^+	11.91 [11]			

(*b*) Interstitial: I(A)

MF_2	A	U (eV)	'On'- or 'off'-site, δ (LU) along ⟨100⟩	Barrier at [000]	Height (eV) along ⟨110⟩
CaF_2	Li^+	−5.360	on	—	—
	Na^+	−4.236	on	—	—
	K^+	−1.342	on	—	—
	Rb	+0.676	on	—	—
SrF_2	Li^+	−5.626	0.135	≈0.015	≈0.003
	Na^+	−4.754	on	—	—
	K^+	−2.576	on	—	—
	Rb	−0.914	on	—	—
$SrCl_2$	Na^+	−4.10 [11]			
	K^+	−2.68 [11]			

3.1.2. Extrinsic defects. Tables 2(*a*) and 2(*b*) concern the 'free' alkali-ion impurities respectively as a substitutional cation S(A) and as an interstitial I(A). The tables display the defect formation energies U in the first results column, then the equilibrium position of the dopant A as either 'on'-site (the centre of the fluorine cube) or 'off'-site, with the displacement δ along the ⟨100⟩ tetragonal axes S_4. In the last two columns the energy barriers are reported at the 0,0,0 'on'-site position and at the saddle-point along the ⟨110⟩ binary axes A_2. Elementary arguments [25] on electrostatic and ion-size effects explain the behaviour of U: the smaller the impurity (ionic radii [19]) or the larger the host-lattice parameter a, the lower the U-value. Similarly the relaxations of the NN ions may be explained [25]: the fluorine displacements are lower than 0.11 LU (S(Rb) in CaF_2) and the 'M' ones are lower than 0.09 LU (I(Rb) in CaF_2). If the impurity ion size is appreciably smaller than the crystal host cation (Li in CaF_2 and SrF_2), its equilibrium position is 'off'-site, particularly in the substitutional configuration. When the substituted ion is small the neighbouring ions have enough room to relax, so they decrease the energy by lowering the local symmetry. In other words, by obvious arguments [25] the 'on'-site position is an unstable equilibrium position with respect to the pure electrostatic interactions, whereas it is stable with respect to SRI. Thus, with both interactions, the 'on'-site equilibrium position becomes stable only if the 'A–F' SRI is large enough; if it is not, the 'stable' equilibrium positions are 'off'-site and break the symmetry. This effect is magnified by the polarisation and distortion of the surrounding

crystal; it would be interesting to check it in 'BaF_2:Li' and 'BaF_2:Na'. Such effects have already been studied in other materials: alkali-doped alkali halides [20, 21] and transition-ion-doped alkaline-earth oxides [22, 23]. Nevertheless we may observe that the barriers separating the symmetry-equivalent off-site wells around the 'on'-site positions are so low (a rather flat energy surface) that the Li dopant probably jumps or tunnels through the barriers (this is the case except perhaps for substitutional Li in SrF_2) even at very low temperatures.

3.1.3. Migration energies. The migration energy ΔU_m of a defect is the minimum energy required to get over the potential barrier separating two neighbouring equivalent stable configurations (SC):

$$\Delta U_m = U(\text{SPC}) - U(\text{SC}).$$

U(SPC) is the formation energy of the defect in the saddle-point configuration (SPC)—that is, the lowest unstable equilibrium configuration between the two neighbouring equivalent SC of the defect, the formation energy of which is U(SC).

Figures 1 describe various SPC. Figure 1(*a*) shows the SPC of a fluorine vacancy migration, figure 1(*b*) shows that of an M vacancy migration and figure 1(*c*) shows the saddle point (SP) of an F or M interstitial ion for the 'direct' mechanism. Figures 1(*d*) and 1(*e*) describe, respectively, the SPC of an F and of an M migrating interstitial for the energetically cheapest 'interstitialcy' mechanism: two F or two M ions are moving together in a correlated way. The full arrows of figures 1 show the effective directions of some ion relaxations.

Table 3 displays the values of ΔU_m for the 'free' intrinsic defects. Clearly, as is well known, the V(F) defect is the most mobile and the 'interstitialcy' mechanism for the I(F) requires much less energy than the 'direct' one, but it probably occurs at much higher temperature than the V(F) motion. In any case, the mobility of the cationic disorder (V(M) and I(M)) is very probably negligible, except perhaps at very high temperatures near the melting point. We may also note that all these migration energies ΔU_m are appreciably smaller than the corresponding formation energies (table 1). Thus all these defects are certainly very mobile at their formation temperatures. We have checked that the SP (figures 1(*a*), (*b*), (*c*)) are very close to the centre of the fluorine cube edge and the NN F ions are pushed away from the edge of the cube to a negligible degree (this has been carefully studied particularly with I(F) 'direct' migration [25]). By comparing the positions of the various relaxed NN ions for the SPC with respect to those for the stable configurations, we see that all the displacements during the migration process are outwards (up to 0.26 LU) in spite of the electrostatic interaction being attractive. Clearly the migration energies are much affected by the choice of the SRI potentials and by their reliability at considerably shorter distances than in the perfect crystal. Thus the low values given by Bendall and co-workers [11] may be perhaps explained either by the choice of SRI or by the large $SrCl_2$ lattice parameter.

Like table 3, table 4 gives the energies of migration ΔU_m of an A interstitial for migration by the simplest process (figure 1(*c*)). Comparing the displacements of the relaxed NN ions in the SPC with respect to the stable configuration [25], the SP is certainly at the middle of the edge of the fluorine cube, because all these ions are largely pushed outwards. The NN fluorines are displaced by a distance in the range from 0.07 LU (SrF_2:Li) to 0.28 LU (CaF_2:Rb) and the NN M^{2+} cations are displaced by about 0.08 LU. Therefore the migration energies are chiefly determined by the short-range repulsive forces (the A ion size), so the ΔU_m (I(A)) results are probably strongly dependent on

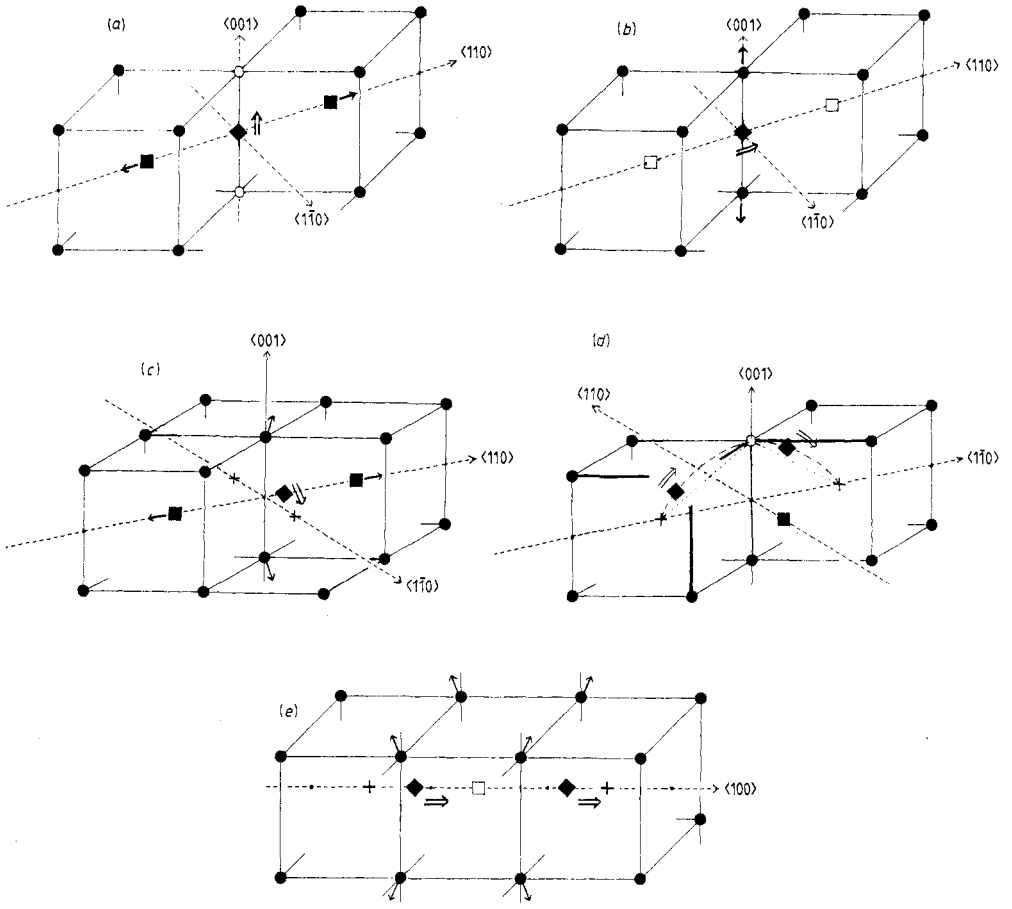

Figure 1. Saddle-point configurations in migrating processes. (*a*) Fluorine vacancy. (*b*) Alkaline-earth vacancy. (*c*) Interstitial from 'direct' migration mechanism. (*d*) Fluorine interstitial from 'interstitialcy' mechanism. (*e*) Alkaline-earth interstitial from 'interstitialcy' mechanism or linear motion of an alkali-interstitial–substitutional pair. ●, F^- ion; ■, M^{2+} ion ; ○, F^- vacancy; □, M^{2+} vacancy; +, interstitial site; →, direction of relaxation of the ions; ◆, ⇑, migrating ion ((*a*), (*d*) F^- ion; (*b*) M^{2+} ion; (*c*) F^-, M^{2+} or A^+ ion; (*e*) M^{2+} or A^+ ion).

Table 3. Migration energies ΔU_m (eV) of intrinsic 'free' defects in 'MF_2' crystals.

MF_2		V(F)	I(F) 'interstitialcy'	I(M) 'interstitialcy'	V(M)	I(F) 'direct'	I(M) 'direct'
CaF_2	This work	0.267	0.811	2.057	2.628	2.992	4.213
	[9]	0.35	0.91				
	[12]	0.27†	0.81†				
SrF_2	This work	0.360	0.756	1.877	2.558	2.982	4.068
	[9]	0.43	0.80				
$SrCl_2$	[11]	0.24	0.46			0.87	

† g_p (extrapolated to 0 K).

Table 4. Migration energies ΔU_m(eV) of 'free' alkali interstitials.

MF_2 \ A	Li^+	Na^+	K^+	Rb^+
CaF_2	1.898	3.328	3.171	2.611
SrF_2	1.440	3.051	3.199	2.712

the choice of the SRI parameters ('A–F' and 'A–M' SRI). For instance, the weakness of the NN M-ion displacements are perhaps spurious, since we have neglected the 'A–M' SRI. Moreover, the use of the SRI (obtained from the experimental properties of 'AF' and 'MF_2' perfect crystals) is rather questionable whenever the geometrical structure of the local disorder is very unlike that of the perfect crystal (ionic distances, coordination numbers, . . .). Nevertheless, by comparing table 3 and 4 we observe that the I(A) defects become mobile at temperatures of the same order of magnitude as or even higher than the intrinsic disorder defects in the cationic sublattice [V(M) and I(M)]. We have not studied the mobility of substitutional alkali: the migration is probably much more energetically expensive for S(A) than I(A), because it requires an exchange between S(A) and M 'on'-site ions by a rather complicated mechanism (creation of a cationic Frenkel pair close to the alkali, for instance). So the A ions are probably 'frozen' at their sites up to very high temperatures. With the smallest impurities A the migration energy increases with the size of A and decreases with the host-lattice parameter; it is not clear whether the calculated behaviour of the larger impurities (K and especially Rb) is physically meaningful, considering the above comments about the reliability of the SRI in migration simulations.

3.2. Clustering of elementary defects

3.2.1. Formation of clusters. Let ΔU_c be the trapping energy of a cluster made up from two elementary defects, X and Y:

$$\Delta U_c = U(X) + U(Y) - U(X{*}Y).$$

$U(X{*}Y)$ is the formation energy of the pair made up of the X and Y defects, close enough to interact. $U(X)$ and $U(Y)$ are the previous (§ 3.1.1. and § 3.1.2) formation energies of the 'free' defects; clearly the X*Y pair defect is stable if ΔU_c is positive. Assuming that at least one defect (X or Y) is sufficiently mobile at the temperature of interest, then the larger the ΔU_c value, the more probable the X*Y cluster. Here we assume the absolute extremum value of ΔU_c is obtained in the closest configuration.

Table 5 gives the values of ΔU_c for an alkali-interstitial–alkali-substitutional pair, [I(A)*S(A)], and the 'off'-site outwards displacement δ of the A ions from their 'on'-site positions (the centres of two adjacent cubes of fluorines) along the [100] tetragonal axis S_4 (figure 2(*a*)). The pair looks like a dumbbell. Clearly, if the alkali-interstitial and alkali-substitutional ions coexist in the 'MF_2:A'-doped crystal, they always tend to cluster together (large ΔU_c-values). We think that these pairs can be created at only rather high temperatures (see § 3.1.3, table 4; large ΔU_m-values), but after they have been created they should be very stable, particularly for Li.

The weaker the A–F SRI potential (approximately, the smaller the A ion size) the more stable the pair, and the more central the dumbbell on the substitutional site. In the 'MF_2:K and Rb' systems the dumbbell is centred on the face of a fluorine cube, whereas in 'MF_2:Li' it is exactly centred at the substitutional site, forming a kind of 'di-substitutional'. The different behaviour of 'MF_2:Li' may be brought about by the

Table 5. Clustering energies ΔU_c and interstitial (δ_I) and substitutional (δ_S) 'off'-site displacements of an [I(A)*S(A)] pair in 'MF_2 : A' crystals; outwards displacements have positive values of δ.

A	MF_2	CaF_2			SrF_2			$SrCl_2$
		ΔU_c (eV)	δ_I (LU)	δ_S (LU)	ΔU_c (eV)	δ_I (LU)	δ_S (LU)	ΔU_c (eV)
Li^+	This work	2.121	−0.551	0.449	2.310	−0.543	0.457	
	[10]	2.17	−0.551	0.449				
Na^+	This work	0.895	−0.091	0.105	0.938	−0.164	0.159	
	[10]	0.89	−0.088	0.101				
K^+	This work	1.127	−0.038	0.093	1.034	−0.056	0.098	
	[10]	1.09	−0.082	0.072				0.62 [11]
Rb^+	This work	1.254	−0.047	0.108	1.170	−0.046	0.132	
	[10]	1.45	−0.128	0.038				0.66 [11]

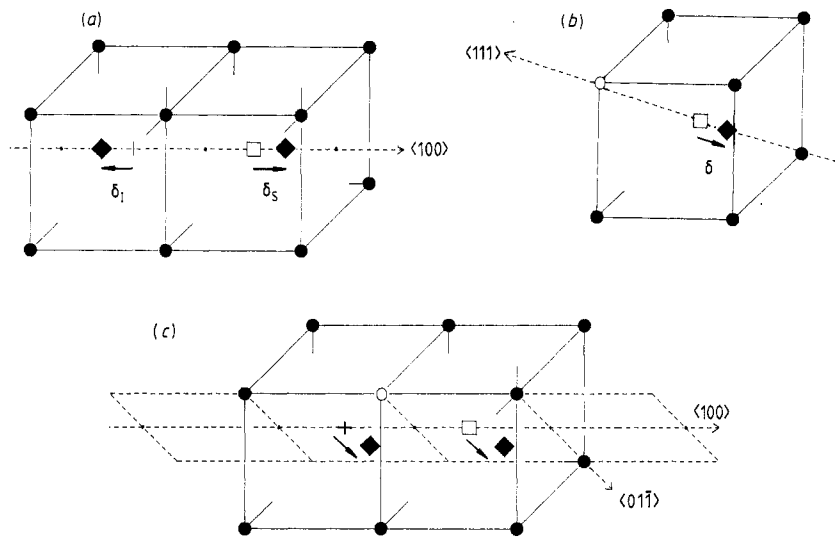

Figure 2. Clusters in 'MF_2 : A' crystals. ◆, A^+ ion; other symbols, see caption of figure 1.

smallness of the 'Li–F' SRI—that is, the Li size is assumed to be considerably smaller than the sizes of the other alkaline ions. This effect of the A ion size is perhaps increased if the host crystal has a large parameter. In table 5, we used the 'Rb–Rb' SRI parameters from [16]. Neglecting these SRI makes the results physically quite aberrant for 'SrF_2 : Rb' and decreases ΔU_c for 'CaF_2 : Rb' by more than 0.30 eV. On the other hand, neglecting the alkali–alkali SRI changes ΔU_c for 'MF_2 : K' by less than 0.06 eV. The 'Li–Li' and 'Na–Na' SRI have a negligible influence on the calculations of ΔU_c, in agreement with what was found by Jacobs and co-workers [10]. This example clearly emphasises the large impact of the choice of SRI, and it reinforces our objections (§ 3.1.3) about the results. Therefore our ΔU_c-results for the heaviest impurities are perhaps questionable.

Similarly, table 6 displays the values of ΔU_c and δ of the fluorine-vacancy–alkali-substitutional pair (figure 2(*b*)) [V(F)*S(A)]; δ is the outwards displacement of the S(A) from the substitutional 'on'-site position along the [111] trigonal axis A_3. All

Table 6. Clustering energies ΔU_c and substitutional 'off'-site displacements of a [V(F)*S(A)] pair in 'MF_2: A' crystals.

A	MF_2	CaF_2		SrF_2		$SrCl_2$
		ΔU_c (eV)	δ (LU)	ΔU_c (eV)	δ (LU)	ΔU_c (eV)
Li^+	This work	1.006	0.178	1.112	0.239	
	[10]	1.00	0.185			
Na^+	This work	0.822	0.071	0.952	0.100	
	[10]	0.80	0.073			
	[12]	0.85†				
K^+	This work	0.759	0.010	0.830	0.045	
	[10]	0.74	0.017			0.61 [11]
Rb^+	This work	0.846	−0.034	0.846	0.014	
	[10]	0.76	−0.024			0.50 [11]

† g_p (extrapolated to 0 K).

these results, particularly the values of δ, may be qualitatively explained [25] by some straightforward arguments about the pure electrostatic interactions and the ion-size effects ('A–F' SRI). Note the good agreements with other results. Clearly, in any case an alkali-substitutional ion traps a fluorine vacancy very easily even at low temperature (low ΔU_m-energy of V(F) migration; table 3). Roughly, the more 'off'-site the substitutional alkali, the easier the trapping; therefore the trapping is easier with a small dopant in a host crystal having a large parameter.

Table 7(*a*) shows the ΔU_c-energies of a fluorine-interstitial–alkali-interstitial pair, [I(F)*I(A)], aligned along a [110] binary axis; this pair is stable and the ΔU_c-values seem to depend rather little on the impurity ion size and on the host crystal. Table 7(*b*) shows that, except for the case of Li^+, an alkali-interstitial–fluorine-vacancy pair [I(A)*V(F)] aligned along a [111] trigonal axis is very unstable. This is to be expected, because the defect charges of I(A) and V(F) are the same. An investigation [25] of the surrounding ion positions shows that the attractive character of [I(Li)*V(F)] results from the inwards displacements of the neighbouring fluorine ions, arising because of the small size of Li (the self-trapping mechanism). Note that the ΔU_c-energy (table 7(*b*)) depends very strongly both on the impurity ion size and on the host-crystal lattice parameter; the 'MF_2: Rb' results are probably spurious (questionable 'Rb–F' SRI; see the comments about tables 3, 4 and 5).

As we shall see in § 3.3, charge compensation when 'MF_2' is doped with 'AF' may proceed either through [I(A)*S(A)] or through [V(F)*S(A)] pairs. If the first process prevailed one could not explain the experimental fact, mentioned in the introduction, that in doped crystals only perturbed colour centres are observed, to the exclusion of the colour centres found in pure 'MF_2'. In an effort to overcome this potential difficulty, one may ask whether the neutral defect [I(A)*S(A)] can trap a fluorine vacancy, leading to a 'perturbed' F centre. The V(F) should be trapped by the electric multipoles of the [I(A)*S(A)] pair and by the self-trapping mechanism (surrounding distortions and polarisations linked to the trio formation: [I(A)*F(A)*V(F)]). Table 8 lists the trapping energy ΔU_c for just one of the possible geometrically closest configurations of the trio (figure 2(*c*)). We have not computed the values for 'MF_2: Rb', because the [I(Rb)* S(Rb)] pair probably does not exist (table 12, later). This trapping should depend strongly on the temperature because of the rather low values of ΔU_c and ΔU_m (V(F)).

Table 7. Clustering energies ΔU_c (eV) of I(A) with I(F) or V(F) in 'MF_2: A' crystals.

(a) Fluorine-interstitial–alkali-interstitial pair, [I(F)*I(A)] A				
MF_2	Li^+	Na^+	K^+	Rb^+
CaF_2	0.580	0.530	0.590	0.600
SrF_2	0.598	0.540	0.544	0.541
(b) Fluorine-vacancy–alkali-interstitial pair, [V(F)*I(A)] A				
MF_2	Li^+	Na^+	K^+	Rb^+
CaF_2	0.537	−1.081	−4.081	−0.003
SrF_2	0.850	−0.527	−2.874	−0.574

Table 8. The trapping energy ΔU_c(eV) for trapping of a fluorine vacancy by an alkali-interstitial–substitutional pair.

	Li^+	Na^+	K^+
CaF_2	0.107	0.131	−0.028
SrF_2	0.274	0.240	0.140

Because of the very low defect symmetry of the trio, the memory size required and the calculation time increase, so we were compelled to reduce the sizes of the regions (90 ions in region I and about 1200 in I + IIA). Moreover, this cluster is so disordered a defect that the various SRI are perhaps questionable. Therefore, the ΔU_c-values of table 8 are moderately reliable. The general trend is towards easier fluorine vacancy trapping when A is small and the host-lattice parameter large.

One further comment may be made on tables 5 to 8: the trapping may be partly quenched, i.e. the clustering processes can be so slowed down by the heights of the various potential barriers that the components have to jump through while they are approaching one another. We plan to study these effects more systematically in the future.

3.2.2. Reorientation of the clusters. The defect clusters discussed so far have several equivalent orientations. To change from one to another at least one of the components of the defect pair must jump through a potential barrier, the height of which (ΔU_m; see § 3.1.3) is a maximum for the SPC. Here we confine ourselves to the two most likely pairs, [I(A)*S(A)] and [V(F)*S(A)] (see § 3.3 and [10, 11]) and to the most obvious reorientation 'paths'.

Firstly, the [I(A)*S(A)] pair can move linearly by 1.0 LU along its tetragonal [100] axis. At the SPC the dumbbell is centred on the perfect-lattice substitutional site (similar to figure 1(e)), the two ions are inside the substitutional cube with 'MF_2: Na' and inside the two adjacent interstitial cubes with 'MF_2: K or Rb'.

Secondly the [I(A)*S(A)] pair can rotate. From studying 'SrF_2: Na' [25] very carefully, we have checked that in the SPC the rotating dumbbell is centred on the perfect-lattice substitutional site and it is aligned along a Sr row ([110] binary axis) (figure 3(a)).

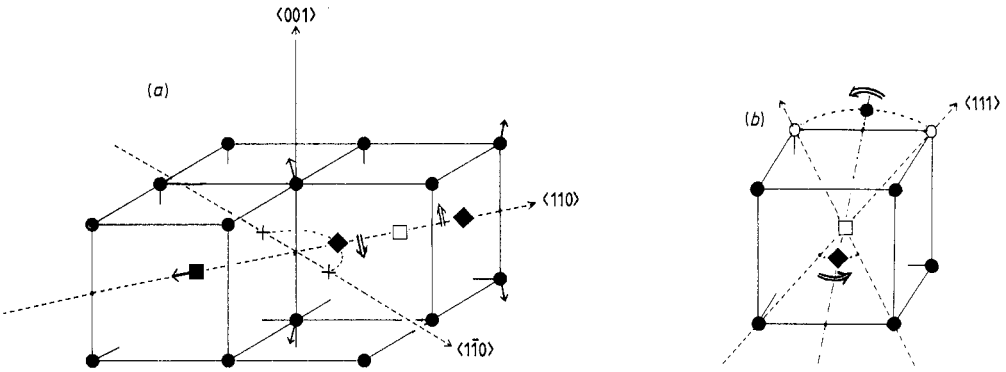

Figure 3. Reorientation of pair defects. (*a*) Rotation of the alkali-interstitial–substitutional pair. (*b*) Rotation of the fluorine-vacancy–alkali-substitutional pair. ◆, ⇑, A^+ migrating ion; ●, ⇑, F^- migrating ion; other symbols, see caption of figure 1.

We assume that the same is true in all the other 'MF_2:A' systems; the two A ions are always inside the substitutional cube, quite close to the cube edges.

Finally, [V(F)*S(A)] can rotate if an NN fluorine ion of the substitutional cube jumps inside the F vacancy. Figure 3(*b*) shows the SPC; the F migrating ion is close to the cube edge, inside or outside the substitutional cube (inside in the case of light 'A' impurities and large host-lattice parameter). We think that the ΔU_m-energies of these three reorientation processes are probably the lowest.

The pair reorientation can be detected by ionic thermocurrent (ITC) and dielectric relaxation (DR) experiments [5, 10] provided that the pair has a sufficient electric dipole momentum (EDM). In table 9 we list rough calculated EDM values of the stable configuration of the defect pairs. These were obtained by neglecting firstly the very small shell polarisations of the ions of the pair, and secondly the polarisations of the neighbouring host crystal (regions I and IIA). Note that the EDM vanishes at the SPC of both [I(A)*S(A)] processes of reorientation described above. The EDM values increase approximately as the impurity ion size, and they depend little on the host crystal. The [I(A)*S(A)] dipoles are aligned along the ⟨100⟩ directions (tetragonal S_4 axis) towards

Table 9. The electric dipole momentum (units: Å electron) of the alkali-interstitial–substitutional pair and of the fluorine-vacancy–substitutional pair.

(*a*) [I(A)*S(A)]				
	A			
MF_2	Li^+	Na^+	K^+	Rb^+
CaF_2	<0.003	2.16	2.37	2.31
SrF_2	<0.003	1.96	2.50	2.38
(*b*) [V(F)*S(A)]				
	A			
MF_2	Li^+	Na^+	K^+	Rb^+
CaF_2	1.87	2.16	2.33	2.45
SrF_2	1.81	2.21	2.37	2.46

Table 10. The activation energies of reorientation ΔU_m (eV) of the alkali-interstitial–alkali-substitutional and fluorine-vacancy–alkali-substitutional pairs.

			A			
			Li^+	Na^+	K^+	Rb^+
(*a*) [I(A)*S(A)] pair: calculated						
CaF_2	Linear	This work	No	0.441	1.500	1.256
	Rotation	This work	0.620	0.828	1.994	1.857
	Rotation	[10]	0.64	0.91	3.02	3.13
SrF_2	Linear	This work	No	0.063	1.068	0.942
	Rotation	This work	0.569	0.482	1.406	1.375
(*b*) [V(F)*S(A)] pair: calculated						
CaF_2		This work	0.395	0.499	0.773	0.934
		[10]	0.40	0.50	0.74	0.93
SrF_2		This work	0.483	0.482	0.678	0.793
(*c*) Experimental						
CaF_2		[10]	0.334	0.38	0.353	0.32
		[10]	0.502	0.522	0.513	0.511
		[5]	0.345	0.504	0.343	0.322
SrF_2		[24]		0.473		
		[6]	0.70	0.458	0.593	0.527

the interstitial, and the [V(F)*S(A)] dipoles are aligned along the ⟨111⟩ directions (trigonal A_3 axis) towards the fluorine vacancy. Note the vanishingly small EDM of the lithium 'di-substitutional' [I(Li)*S(Li)] in both CaF_2 and SrF_2; such a pair cannot be detected by the ITC or DR techniques.

Table 10 displays the calculated 'reorientation' energies ΔU_m of the [I(A)*S(A)] pair (linear motion, rotation) and [V(F)*S(A)] pair (rotation). The bottom of the table is devoted to the activation energies deduced from analyses [5, 6, 10, 24] of the ITC and DR experiments. Our Li and Na values agree fairly well with those calculated by Jacobs and co-workers [10], but the heavy (K or Rb) [I(A)*S(A)] pairs—perhaps [V(F)*S(A)] too—are somewhat questionable, because of the probably poor reliability of the SRI. For instance, if we neglect the 'A–A' SRI (as is usual with Li or Na), the K results (and, *a fortiori*, Rb ones) become entirely meaningless. The differences between the parameter choices do not completely explain the discrepancies between our calculated K and Rb results and those of Jacobs and co-workers. The calculated (i) 'CaF_2: K and Rb' and (ii) 'SrF_2: Rb' results differ substantially from the 'experimental' ones, which probably again exhibits the weakness of the model (SRI choices in mixed materials with a geometrical structure of defects too far from the perfect-lattice geometry). For the other crystals the calculated and 'experimental' ΔU_m-values match rather poorly, and consistent conclusions are not obvious. This is firstly because of the dispersion of the experimental results, secondly because of the difficulties in the analyses of ITC and DR experiments, and thirdly because of the calculation assumptions. Therefore it is not clear at all which pair (either [I(A)*S(A)] or [V(F)*S(A)]) is observed in 'MF_2: Li' and 'MF_2: Na' crystals. Furthermore, the calculated [I(Li)*S(Li)] should not be detected by ITC or DR (vanishing dipoles; table 9), even with 'SrF_2: Li'. From comparing the orders

of magnitude (table 10), we see that the [V(F)*S(A)] are probably the observed pairs in 'MF_2: K or Rb'. The calculated ΔU_m-energies of the [I(A)*S(A)] and [V(F)*S(A)] pairs are lower than the ΔU_c-energies (tables 5 and 6) in the 'MF_2: Li or Na' crystals, so these pairs probably do not dissociate when reorientating. On the other hand, in 'MF_2: K or Rb' the ΔU_m and ΔU_c are comparable and the pairs may dissociate partly while reorientating. We think, however, that the ΔU_m reorientation energies should be compared with the heights of the first potential barriers of the dissociation process rather than with the pair formation ΔU_c-energies. Therefore in 'MF_2: K or Rb' (and perhaps for [I(Na)*S(Na)] of 'CaF_2: Na') the reorientation processes are probably much more complicated than the ones considered above (and depicted in figures 3(*a*), 3(*b*) and 1(*e*)).

3.3. Solution of alkali halides into alkaline-earth fluorides

3.3.1. Modes of solution. Following Bendall and co-workers [11], we study five modes of solution of an 'AF' crystal into an 'MF_2' crystal, assuming that the 'AF' concentration is small enough that the defects formed do not interact.

(i) Mode 'a'. The A alkali substitutes for an M alkaline-earth (S(A) defect), a fluorine vacancy V(F) is created and a new cell of the 'MF_2' host crystal is formed; it may be symbolised by the following reaction:

$$\{MF_2\}_n + AF \rightarrow V(F) + S(A) + \{MF_2\}_{n+1}.$$

The solution energy ΔU_s is the energy absorbed by the 'MF_2–AF' mixing to get the defects into 'MF_2: A' doped crystal. ΔU_s is given by

$$\Delta U_s(a) = U[V(F)] + U[S(A)] + U_{coh}(MF_2) - U_{coh}(AF)$$

where $U[X]$ is the formation energy of the defect X, and $U_{coh}(MF_2)$ and $U_{coh}(AF)$ are the cohesive energy of the alkaline-earth fluoride and that of the alkali fluoride. According to the notation of the HADES2 program, $U_{coh}(MF_2)$ or $U_{coh}(AF)$ is the required energy to form a new cell of the MF_2 or AF crystal from the distant ions (M^{2+}, F^-, A^+); so our U_{coh} values are always negative. Clearly the V(F) and S(A) 'free' defects can cluster together into a pair (§ 3.2.1) and the energy $\Delta U_s(a)$ becomes

$$\Delta U_s'(a) = U(V(F)*S(A)) + U_{coh}(MF_2) - U_{coh}(AF).$$

(ii) Mode 'b'. Two 'AF' molecules of an alkali fluoride crystal are melted into 'MF_2' giving rise to an A interstitial ion, an A substitutional ion and a new 'MF_2' host crystal cell:

$$\{MF_2\}_n + 2AF \rightarrow I(A) + S(A) + \{MF_2\}_{n+1}.$$

Like Bendall, we normalise the solution energies ΔU_s and $\Delta U_s'$ at a constant concentration of the A impurity ion, whatever the type of defect created. Thus,

$$\Delta U_s(b) = \tfrac{1}{2}U[I(A)] + \tfrac{1}{2}U[S(A)] + \tfrac{1}{2}U_{coh}(MF_2) - U_{coh}(AF).$$

Taking into account the possible interstitial–substitutional clustering we get

$$\Delta U_s'(b) = \tfrac{1}{2}U[I(A)*S(A)] + \tfrac{1}{2}U_{coh}(MF_2) - U_{coh}(AF).$$

We think that Jacobs and co-workers [10] do not use this normalisation; therefore their energies for reaction (b) ([I(A)*S(A)]) are approximately twice ours. Thus comparing their own non-normalised energies $\Delta U_s(a)$ and $\Delta U_s(b)$ they draw inferences that are

Table 11. Formation energies ΔU_s (eV) of 'MF_2 : A' crystals according to the various modes of reaction without defect clustering. (The values in parentheses are from [10], including normalisation correction for reaction b; see text.)

	A							
	Li^+		Na^+		K^+		Rb^+	
	Mode	ΔU_s	Mode	ΔU_s	Mode	ΔU_s	Mode	ΔU_s
CaF_2	b	1.741 (1.73)	b	1.284 (1.165)	a	2.147 (1.92)	a	3.058 (2.35)
	a	2.649 (2.63)	a	1.916 (1.79)	b	2.200 (1.955)	b	3.465 (2.82)
	e	3.597	c	3.239	c	3.463	c	4.374
	d	3.732	e	3.417	e	5.017	d	4.813
	c	3.965	d	3.552	d	5.151	e	6.638
SrF_2	b	1.856	b	1.228	b	1.544	b	2.469
	e	2.993	a	2.263	a	2.012	a	2.596
	a	3.087	e	2.562	c	3.012	c	3.595
	d	3.581	d	3.149	e	3.445	e	4.710
	c	4.087	c	3.262	d	4.032	d	5.298
$SrCl_2$	[11]		b	0.81	b	1.20		
			a	1.32	a	1.32		
			c	2.25	c	1.89		
			d	2.30	d	3.07		
			e	2.36	e	3.13		

different to ours. We list in our tables 11 and 12 Jacobs and co-workers' values after including the factor of $\frac{1}{2}$ for the normalisation.

(iii) Mode 'c'. Two 'AF' molecules become two alkali substitutionals, one alkaline-earth interstitial and one new host crystal cell:

$$\{MF_2\}_n + 2AF \rightarrow 2S(A) + I(M) + \{MF_2\}_{n+1}$$

and, normalising $\Delta U_s(c)$,

$$\Delta U_s(c) = U[S(A)] + \tfrac{1}{2}U[I(M)] + \tfrac{1}{2}U_{coh}(MF_2) - U_{coh}(AF).$$

In this case we have not studied any associated cluster because we shall see that this reaction is very unlikely. Besides, the final cluster should probably be an [I(A)*S(A)] pair, as in mode b, after an exchange between S(A) and I(M) 'free' defects (assuming them to be mobile during the doping process).

(iv) Mode 'd'. Similarly to the above:

$$\{MF_2\}_n + 2AF \rightarrow 2I(A) + V(M) + \{MF_2\}_{n+1}$$

and

$$\Delta U_s(d) = U[I(A)] + \tfrac{1}{2}U[V(M)] + \tfrac{1}{2}U_{coh}(MF_2) - U_{coh}(AF).$$

By similar arguments to the above, no cluster has been studied.

(v) Mode 'e'. The 'AF' solution gives an A interstitial and an F interstitial:

$$AF \rightarrow I(F) + I(A) \qquad \Delta U_s(e) = U[I(F)] + U[I(A)] - U_{coh}(AF)$$

and with clustering

$$\Delta U_s'(e) = U[I(F)*I(A)] - U_{coh}(AF).$$

In tables 11 and 12, the solution energies ΔU_s(mode) and $\Delta U_s'$(mode) are listed in

Table 12. Formation energies $\Delta U_s'$ (eV) of 'MF_2: A' crystals according to the various modes of reaction with defect clustering. (The values in parentheses are from [10], including normalisation correction for reaction b; see text.)

	A							
	Li^+		Na^+		K^+		Rb^+	
	Mode	ΔU_s	Mode	ΔU_s	Mode	ΔU_s	Mode	ΔU_s
CaF_2	b	0.680 (0.645)	b	0.837 (0.72)	a	1.388 (1.18)	a	2.211 (1.59)
	a	1.643 (1.63)	a	1.094 (0.99)	b	1.635 (1.42)	b	2.839 (2.095)
	e	3.017	e	2.887	c†	3.463	c†	4.374
	d†	3.722	c†	3.239	e	4.427	d†	4.813
	c†	3.965	d†	3.552	d†	5.151	e	6.038
SrF_2	b	0.701	b	0.759	b	1.027	a	1.750
	a	1.975	a	1.311	a	1.182	b	1.884
	e	2.395	e	2.022	e	2.900	c†	3.595
	d†	3.581	d†	3.149	c†	3.012	e	4.169
	c†	4.087	c†	3.262	d†	4.032	d†	5.298

† Without clustering; see text.

order of increasing values (i.e. probably in order of decreasing probabilities), for each 'MF_2: A' system. In table 11 the defects are assumed to be 'free' and in table 12 'clustered' (other than for modes c and d); we also report '$SrCl_2$: A' values from [11] and corrected values from [10] for 'CaF_2: A'.

3.3.2. Comments. Looking at tables 11 and 12, the two most probable solution reactions are the a and b modes. Moreover, the smaller the dopant ion size and the larger the alkaline-earth host, the more favoured the b mode. Clustering does not characteristically modify these qualitative results. Free or clustered alkali-interstitial and alkali-substitutional defects alone should be observed in 'CaF_2: Li', 'SrF_2: Li' and 'SrF_2: Na' materials and the I(A) and S(A) in 'CaF_2: Na' and 'SrF_2: K' if we assume the created defects are free (reaction b). Free or clustered fluorine vacancies and alkali substitutionals alone should be created in 'CaF_2: Rb' (reaction a). In all the other materials the solution energies ΔU_s ($\Delta U_s'$) of the a and b reactions are too close, so the two reactions probably coexist with various weights according to the alkali impurity, the host crystal and the 'free' or 'clustered' state of the created defects. In these doubtful situations, the choice of the model parameters (SRI and SM) and of the approximations (thermodynamic ones, for instance) and assumptions (see below) can probably change even the sign of the energy differences $\Delta U_s(a) - \Delta U_s(b)$ and $\Delta U_s'(a) - \Delta U_s'(b)$. For '$MF_2$: Li' these conclusions are somewhat inconsistent with ITC or DR results (§ 3.2.2). A better agreement would perhaps be restored either by using a more suitable defect simulation (SRI choices, thermodynamic effects) or by performing a more sophisticated analysis of the experiments, or by making both improvements together. The agreement with the corrected theoretical values given by Jacobs and co-workers is fairly good; we think that the quantitative deviations originate from the different choices of the parameters (SRI, SM and the region sizes).

4. Conclusions

The principal results of this theoretical study are the following. When doping an alkaline-earth fluoride crystal with alkali fluorides, clustered pairs of interstitial–substitutional

impurities are formed with the smallest alkali ions, but with the largest ones there are clustered pairs of fluorine vacancies and substitutional impurities. Also the [I(A)*S(A)] pairs can weakly trap a fluorine vacancy. Except for the theoretically predominant 'Li di-substitutional' [I(Li)*S(Li)] pair, all the defect pairs exhibit an electric dipole in the ⟨100⟩ direction ([I(A)*S(A)] pair) or in the ⟨111⟩ direction ([V(F)*S(A)] pair). In an electric field they give reorientation signals that are more or less theoretically understood. The alkali impurities are probably quite immobile. Throughout this study we have shown the important role of the relative sizes of the impurity ion and of the host-crystal parameter, particularly when the ions are displaced through large distances.

There are two weak points in our calculations: first, a thermodynamic problem, and, secondly, the choice of model parameters. As we pointed out previously, our results (U-, ΔU-energies and ion displacements) are strictly computed only for 0 K and a constant crystal volume. It would probably be much better to calculate g_p, the free Gibbs enthalpy at constant pressure, for various temperatures in order to approximate the experimental conditions more closely. Furthermore, the temperature dependence of U and ΔU and the entropy contributions may substantially modify our results. Another difficult topic arises: certainly at very low and probably at room temperature, the various observed defects are out of thermodynamic equilibrium. To reach equilibrium, all the defects or their components (during clustering or the defect formation reaction) must be able to migrate at the temperature considered. If the migration potential barriers are too high at the effective crystal temperature T, then the distribution of the defects is 'frozen' as an equilibrium distribution of a higher temperature T_f: but what is the T_f-value?

Finally we have strongly emphasised the important contribution of the ion-size effects—that is to say, the choice of the short-range potential parameters. As they are fitted to the perfect-lattice properties, they are suitable only in so far as the defective crystal configuration is not too different from the perfect one. How good are they when applying them to the substantially displaced nearest-neighbouring ions around the defect? How accurate is the use of the alkali fluoride parameters for the 'A–F' interaction in A-doped alkaline-earth fluoride? (In 'MF_2:A', both the 'A–F' distances and the A coordination number are often very different to the 'AF' perfect crystal.) Neglecting the alkali–alkaline-earth short-range repulsive interactions is probably questionable for the largest impurities (K, Rb). All these approximations may be poor, particularly when calculating migrations, clusterings or defect reorientations.

In the future we will try to study some of the above-mentioned topics, e.g. thermodynamic effects and SRI parameter choice. We shall also extend these calculations to the alkali-doped BaF_2 crystal in order to improve our understanding of the host-crystal effects.

Acknowledgments

The authors are grateful to the AERE (Harwell, UK) for providing the HADES2 code; one of us (MT) is particularly grateful to A M Stoneham and A H Harker (AERE) for introduction to this kind of problem and their helpful advice. We are also grateful to C R A Catlow, A V Chadwick, J J Fontanella and E Laredo for their comments and suggestions made during the ICDIC conference (Parma, Italy, August–September 1988) where the present work was briefly reported.

References

[1] Doualan J L, Margerie J, Martin-Brunètiere F and Rzepka E 1983 *J. Physique Lett.* **44** L375
Tijero J M G and Casas-Gonzales J J 1985 *J. Physique Lett.* **46** L861

[2] Chadwick A V and Terenzi M (ed.) 1985 *Defects in Solids* (London: Plenum)
[3] Catlow C R A and Mackrodt W C (ed.) 1982 *Computer Simulations of Solids* (Berlin: Springer)
[4] Fontanella J J, Wintersgill M C and Andeen C G 1980 *Phys. Status Solidi* b **97** 303
[5] Fontanella J J, Chadwick A V, Carr V M, Wintersgill M C and Andeen C G 1980 *J. Phys. C: Solid State Phys.* **13** 3457
[6] Wintersgill M C, Fontanella J J, Saghafian R, Chadwick A V and Andeen C G 1980 *J. Phys. C: Solid State Phys.* **13** 6525
[7] Fontanella J J, Wintersgill M C, Chadwick A V, Saghafian R and Andeen C G 1981 *J. Phys. C: Solid State Phys.* **14** 2451
[8] Franklin A D 1967 *J. Am. Ceram. Soc.* **50** 648
[9] Catlow C R A, Norgett M J and Ross T A 1977 *J. Phys. C: Solid State Phys.* **10** 1627
[10] Jacobs P W M, Ong S H, Chadwick A V and Carr V M 1980 *J. Solid State Chem.* **33** 159
[11] Bendall P J, Catlow C R A and Fender B E F 1981 *J. Phys. C: Solid State Phys.* **14** 4377
[12] Harding J H 1985 *Phys. Rev.* B **32** 6861
[13] Norgett M J 1974 *UKAEA Report* AERE-R7650
[14] Mott N F and Littleton M J 1938 *Trans. Faraday Soc.* **34** 485
[15] Dick B G Jr and Overhauser A W 1958 *Phys. Rev.* **112** 90
[16] Catlow C R A, Diller K M and Norgett M J 1977 *J. Phys. C: Solid State Phys.* **10** 1395
[17] Catlow C R A and Norgett M J 1973 *J. Phys. C: Solid State Phys.* **6** 1325
[18] Lidiard A B 1974 *Crystals with the Fluoride Structure* ed. W Hayes (Oxford: Clarendon)
[19] Shannon R D 1976 *Acta Crystallogr.* A **32** 751
[20] Catlow C R A, Diller K M, Norgett M J, Corish J, Parker B M C and Jacobs P W M 1978 *Phys. Rev.* B **18** 2739
[21] Sangster M J L 1980 *J. Phys. C: Solid State Phys.* **13** 5279
[22] Sangster M J L and Stoneham A M 1981 *Phil. Mag.* B **43** 597
[23] Rowell D K and Sangster M J L 1982 *J. Phys. C: Solid State Phys.* **15** L317
[24] Ong S H and Jacobs P W M 1979 *Can. J. Phys.* **57** 1031
[25] Amara A 1989 *Thèse Université* Université de Caen